Radial Intensity Profiles of Galactic Cosmic Rays in the Outer Heliosphere

R.A. Caballero-Lopez[1], F.B. McDonald[1], and H. Moraal[2]
(1) Institute for Physical Sciences and Technology, University of Maryland, USA
(2) School of Physics, Potchefstroom University, Potchefstroom, South Africa

Abstract

This contribution describes our understanding of galactic cosmic ray (GCR) proton (H) and α particle (He^{++}) intensities during the solar minimum conditions of 1987 and 1977/1997, with emphasis on the radial profiles in the outer heliosphere. This is done with a model that contains all the relevant physics of the solar wind termination shock with its acceleration and shock drift effects, the appropriate heliosheath modulation, drifts in the heliospheric magnetic field (HMF), as well as drifts along a wavy neutral sheet in the ecliptic plane.

1. Introduction

Steenkamp (1995) and Steenberg (1998) developed a numerical solution of the cosmic ray transport equation

$$\partial f/\partial t + \mathbf{V}\cdot\nabla f - \nabla(\mathbf{K}\cdot\nabla f) - (1/3)(\nabla\cdot\mathbf{V})\partial f/\partial \ln p = Q \qquad (1)$$

where **V** is the solar wind velocity and **K** is the diffusion tensor containing elements describing diffusion along the field, perpendicular to it, as well as gradient and curvature drifts. Steenberg and Moraal (1996, 1999), Moraal *et al.* (1999) and Steenberg *et al.* (1999) applied this solution to several aspects of observed cosmic ray intensities. Steenberg (1998) made a comprehensive fit to the 1977, 1987, and 1997 spectra of GCR H and He^{++}, as well as anomalous cosmic ray (ACR) H, He^{+}, and O^{+}. In this paper we present a subset of these solutions in which we try to find a better set of transport parameters, and we also stronger emphasize the radial and latitudinal distribution, especially across the shock.

2. The Heliospheric Model

The solution is for an azimuthally symmetric heliosphere, consisting of two regions, an inner heliosphere up to the solar wind termination shock (SWTS), and a heliosheath up to the heliopause, where we assume that the undisturbed interstellar spectra (LIS) of GCRs feed the system. The particles experience gradient and curvature drift in HMF, neutral sheet drift along the wavy sheet

pp. 3827–3830

that separates Northern and Southern fields, as well as the appropriate shock drift effects. The solution is started with the initial condition that the LIS pervades the entire heliosphere, and is stepped forward in time until it reaches a quasi-steady state after 8000 time steps of 2.6 hours each ($\approx$ 2.4 years). Since we only study GCR modulation in this contribution, there are no sources inside the heliosphere, and $Q = 0$ in (1). The LIS for GCR H and He^{++} were taken from Webber and Lockwood (2001) as $j_b(\mathrm{H}) = 21.1E^{-2.8}/(1+5.85E^{-1.22}+1.18E^{-2.54})$ and $j_b(\mathrm{He}^{++}) = 1.075E^{-2.8}/(1+3.91E^{-1.09}+0.90E^{-2.54})$.

The primary aim of this paper is to find a set of transport parameters that explains the observed intensities. These parameters are: The SWTS and the heliopause are placed at $r_s = 90$ AU and r_b= 120 AU, respectively. The radial solar wind velocity is $V = 400$ km/s in the ecliptic regions, increasing to 800 km/s about the poles. It falls to 100 km/s at $r = r_s$ and decreases as $1/r^2$ in the heliosheath. The HMF is a Parker spiral, $B = B_e(r/r_e)^2/(\sqrt{2}\cos\psi)$, with $B_e = 5$ nT, and $\tan\psi = (\Omega r \sin\theta)/V$. It is increased by a factor of four above the poles as in the Jokipii and Kota (1989) modification. The wavy neutral sheet has a tilt angle $\alpha = 10°$. Finally, the spatial and rigidity dependence of the diffusion mean free paths $\lambda_\parallel$ and $\lambda_\perp$ ($\lambda = 3\kappa/v$) that fit the spectra best are shown in panels I and J of Figure 1, and are given by:

$$\lambda_\parallel = 0.108 f_i(r) g(\theta) h(P)/(\cos^2\psi + 0.01\sin^2\psi)\ \mathrm{AU}, \quad \lambda_\perp = 0.01\lambda_\parallel,$$

$$g(\theta) = 1, \quad h(P) = P \text{ if } P \geq 0.4 \text{ GV, and } h(P) = 0.4 \text{ if } P < 0.4 \text{ GV}$$

$$f_i(r) = a_i f_{i-1}(r_{i-1})(r/r_{i-1})^{c_i}, \quad r_i < r \leq r_{i+1}, \quad f_0(r_0) = 1, \quad i = 1, 4$$

$$r_0 = 1 \text{ AU}, \quad r_1 = 30 \text{ AU}, \quad r_2 = 70 \text{ AU}, \quad r_3 = r_s, \quad r_4 = r_b$$

$$a_1 = 1, \quad a_2 = 1, \quad a_3 = 1, \quad a_4 = 0.25, \quad c_3 = 0, \quad c_4 = -2$$

$$c_1 = 0.2(qA > 0) = 0.3(qA < 0), \quad c_2 = -2(qA > 0) = 0.7(qA < 0)$$

3. Results

Panels A, B, C and D of Figure 1 show the solutions for the 1977/1997 $qA > 0$ solar minima, and panels E, F, G and H for the 1987 $qA < 0$ solar minimum. Steenberg (1998) concentrated on the format of panels A, B, E, and F; here we emphasize the radial dependence in panels C, D, G and H to show the acceleration at the shock and the modulation in the heliosheath. Panel C shows that the $qA > 0$ calculations fit the observations in the inner heliosphere well, but that the 1997 observed intensities at Voyager 1 (70 AU) and Voyager 2 (57 AU) fit the full line radial profile for the ecliptic plane, rather than the dashed line for 30° North and South respectively. This is due to the large positive latitudinal gradients in the solutions, which we have not been able to reduce. In the $qA < 0$ period of 1987 in Panels G and H, the radial gradients are larger, and the latitudinal gradients are negative w.r.t. the ecliptic plane, as is well-established. In this case, however, the calculated negative latitudinal gradient is less than observed by Voyager 1 (at 31 AU, 34° N).

Panel C shows the shock/heliosheath effect best. It predicts that the ecliptic intensity of 175 MeV (0.6 GV) H (full line) should rise rapidly immediately in front of the shock, but that at other latitudes this jump will only occur beyond the shock. For the 265 MeV/n (1.5 GV) He^{++} in panel D, the effects of the shock and the heliosheath are similar but smaller. In the $qA < 0$ solutions of panels G and H the shock/heliopause effects seem smaller than in the $qA > 0$ case.

Panels K and L show the equivalent H solutions of panels C and G for a heliosphere with the same size as previously, where the modulation parameters inside the shock are the same, but where there is no shock, so that the solar wind continues as inside the shock, and where $f_4 = f_3$ in the parameters above. The solutions are somewhat lower than those that contain the shock, but the radial and latitudinal profiles are quite similar. These panels thus demonstrate that the solutions inside the SWTS are rather insensitive to the effects of the shock acceleration and the heliopause. Furthermore, the solutions beyond $r = 90$ AU do also not differ dramatically, whether this region is a heliosheath beyond the SWTS, or merely an extended modulation region inside the outer boundary.

4. Conclusions

The comparison between shock and no-shock solutions give a quantitative picture of SWTS acceleration and heliosheath effects. These effects are not dramatic. In particular, we notice that the discontinuous jump of B across the shock, which causes a "magnetic wall" in the heliosheath, does not cause an accompanying modulation barrier there, because the fundamental modulation scale lengths $\kappa_{\|}/V$, $\kappa_{\perp}/V$ and κ_T/V do *not* jump discontinuously across the shock. In a more extended version of this work the same analysis will be repeated for solar maximum conditions, and ACRs will be included.

5. References

1. Jokipii, J.R, and Kota, J. 1989, *Geophys. Res. Lett.*, **16**, 1
2. Moraal, H., Steenberg, C.D. and Zank, G.P. 1999, *Adv. Space Res.*, **23**, 425
3. Steenberg, C.D., and Moraal, H. 1996, *Ap. J.*, **463**, 776
4. Steenberg, C.D. 1998, Ph.D. thesis, Potchefstroom University
5. Steenberg, *et al.* 1999, *Proc. 26th ICRC*, **7**, 593
6. Steenberg C.D., and Moraal, H. 1999, *J. Geophys. Res.*, **104**, 24879
7. Steenkamp, R. 1995, Ph.D. thesis, Potchefstroom University
8. Webber, W.R., and Lockwood, J.A. 2001, *J. Geophys. Res.*, **106**, 29323

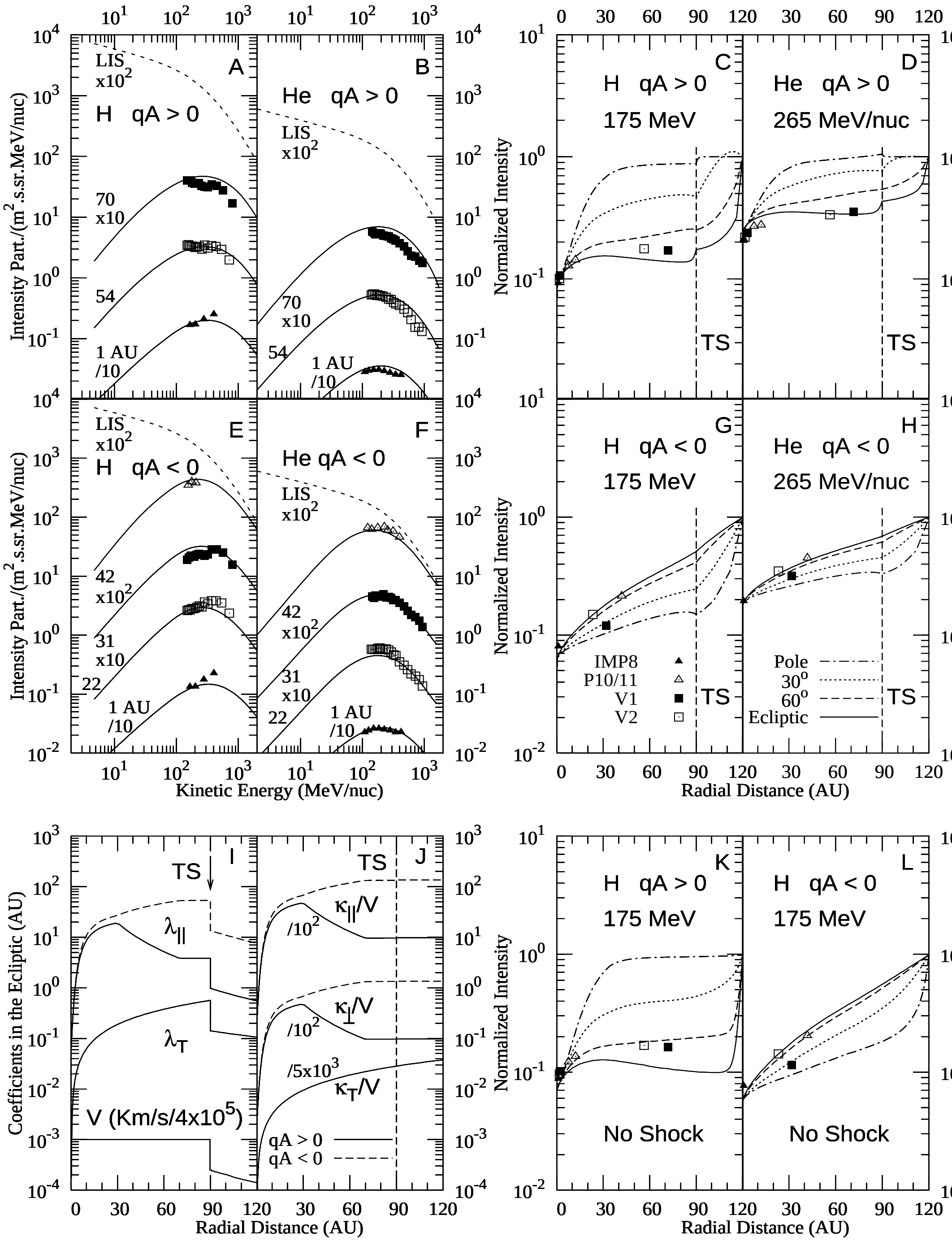

Fig. 1. Modulation of GCR H and He^{++} in the inner heliopsphere and in the heliosheath, including acceleration at the SWTS. PanelsI and J show the parameters used, while panels K and L show the equivalent no-shock solutions for comparison. Voyager data were made available by the Voyager CRS team (P.I.: E.C. Stone).